Thin walled pottery from Alife (Northern Campania, Italy)

Celestino Grifa[1], Alberto De Bonis[2], Vincenza Guarino[2], Chiara Maria Petrone[3], Chiara Germinario[1], Mariano Mercurio[1], Gianluca Soricelli[4], Alessio Langella[1] and Vincenzo Morra[2]

[1] Dipartimento di Scienze e Tecnologie, Università degli Studi del Sannio,
Via Dei Mulini 59/a, 82100, Benevento, Italy
[2] Dipartimento di Scienze della Terra, dell'Ambiente e delle Risorse, Università degli
Studi di Napoli Federico II, Via Mezzocannone 8, 80134, Napoli, Italy
[3] The Natural History Museum, Department of Earth Sciences, Cromwell Road, SW7 5BD London, United Kingdom
[4] Dipartimento di Scienze Umanistiche, Sociali e della Formazione, Università degli Studi del Molise, Isernia, Italy
Corresponding author: *celestino.grifa@unisannio.it*

Abstract

The ancient town of *Allifae* (modern Alife) represents one of the most interesting settlements of the Northern Campania area that, together with the ancient city of *Cales*, was a thriving production centre of pottery. Excavations carried out inside the city wall, near the south gate, the so-called Porta Fiume, unearthed a huge dump of thin walled ware where the most abundant forms were cups and beakers, decorated with grooves or rouletting. The dump has been dated Augustan/ early Tiberian age (20 b.C.- 20 AD) and the thin walled vessels found can be identified with similar wares from *Allifae, Cubulteria*, *Caiatia* and perhaps *Neapolis*. Horace in his *Sermones* (*II, 8,39*) cited the *Allifana* beakers (described as *fictiles ac subtiles* by a Horace scholiast) and they could possibly be identified with the thin walled wares produced in *Allifae*. If this the case, then the thin walled vessels produced in *Allifae* were known in Rome as early as the end of I century B.C. In order to investigate and characterise the *Allifae* thin-walled pottery, twenty-one samples were selected and mineralogical-petrographic analyses (OM, XRPD, XRF and SEM/EDS) were carried out. The clayey raw material used was a low-CaO alluvial clayey deposit from the Middle Valley of the Volturno River. The potters probably handled the sediment by a levigation process in order to remove the coarser grains, and making the clay suitable to produce such thin walls. Comparison with other regional production of thin-walled pottery allowed us to strictly distinguish the *Allifana* beakers.

Key words: Thin walled pottery; Alife; Volturno river clays; Grain Size Analyses; levigation.

Introduction and archaeological background

An archaeological excavation was carried out in 1981 in *Allifae* (modern Alife, Northern Campania, Figure 1), near the Southern gate of the Roman town (the so-called "Porta Fiume"). In addition to a large group of other fine and coarse wares, the excavation yielded a large dump of thin walled pottery (hereafter TW), with numerous overfired and deformed fragments, that would suggest the presence of a pottery-kiln of this fine-ware in its immediate vicinity. The typological comparison of pottery with other regional sites and fine-wares that composed the dump, suggest a date for this deposit as being between the Augustan and early Tiberian age (20 b.C - 20 AD).

The macroscopic aspect of the body appears quite distinctive: it is a quite granular body, varying in colour from orange to dark grey with somewhat rough surfaces and a moderate occurrence of tiny non-plastic inclusions.

Two forms were predominantly abundant in this dump: a carinated cup and a deep hemispherical cup. The carinated cup (Figure 2a-c) is similar to the Marabini XXXIII form (Marabini Moevs, 1973; cf. Mayet, 1975, form XII, n. 167). The examples from *Allifae* are characterised by one or more grooves just above the *carina* and at mid-height of the wall and concentric grooves on the outside of the flat base. The wall may have a slight rouletting decoration with thin vertical (sometimes oblique) lines. There seems to be a relatively constant ratio between the diameters of the rim (between 7 and 10 cm) and the bottom (approximately 1.6:1) and between the overall height of the cup and the rim diameter (about 1:1). Similar vessels
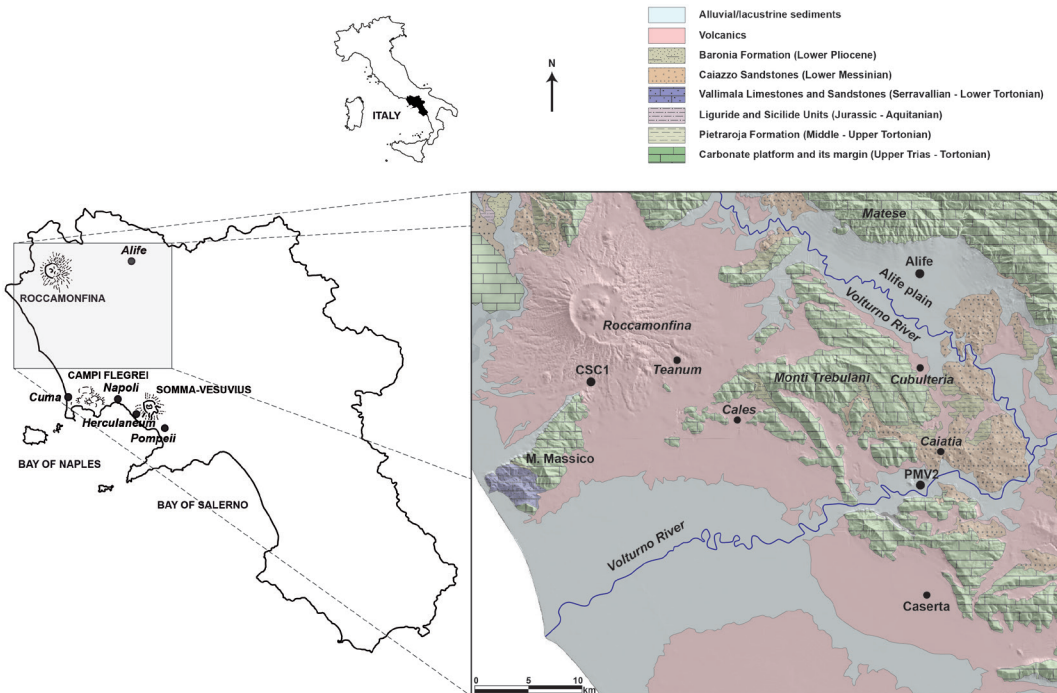
Figure 1. Geological sketch map of the Northern Campania area (modified after Bonardi et al., 2009).
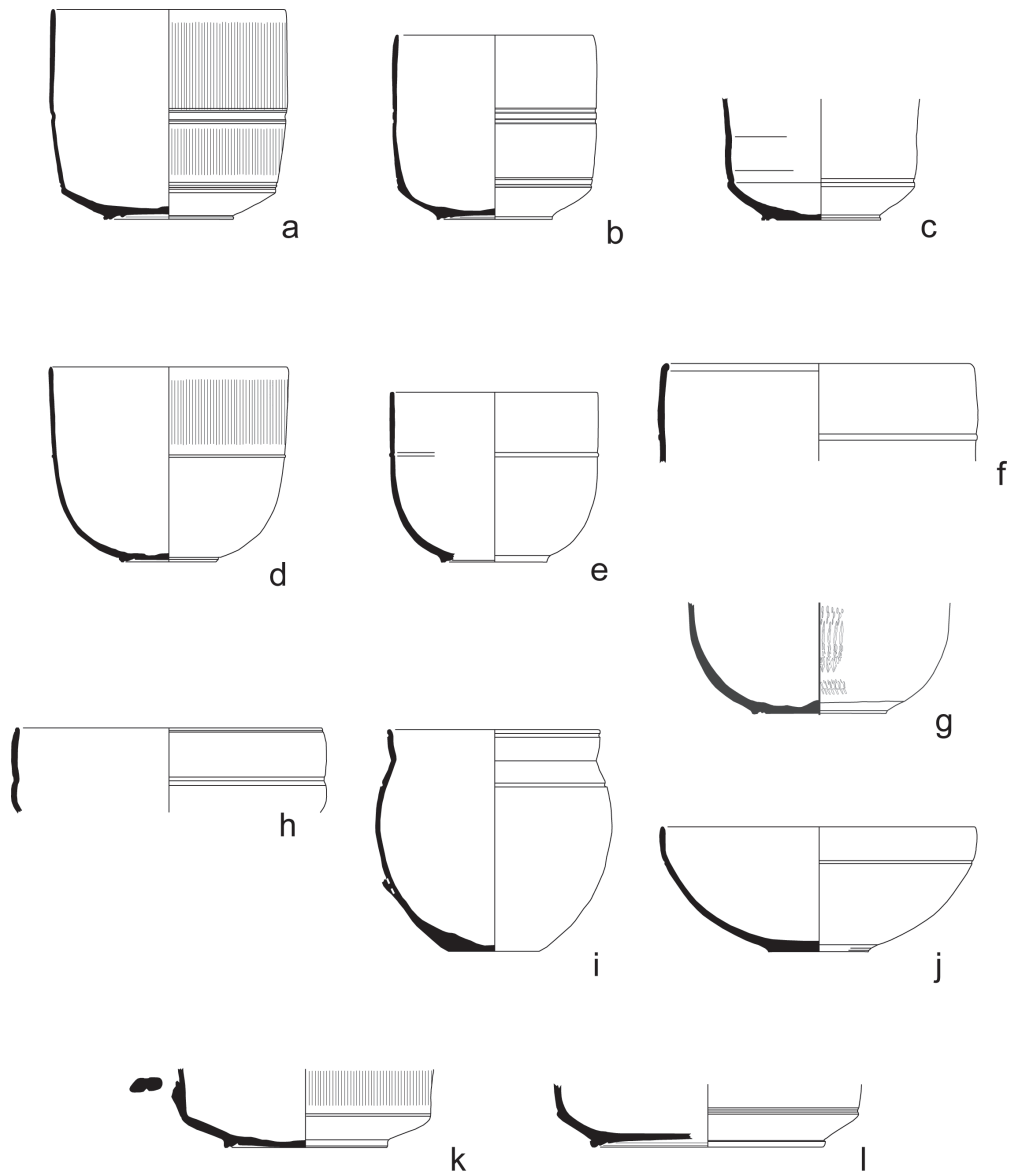
Figure 2. Main forms of TW pottery from Alife; a), b) and c) carinated cup. Marabini XXXIII; d), e) and f) deep hemisferical cup. Marabini XXXVI; g) one-handled globular jug. Marabini LI; h) cup; Marabini XXXVI; i) and j) beaker; Ricci 1985. type 1/164; k) and l) shallow hemispherical bowl.

were found in a Roman villa in the territory of neighbouring *Caiatia* (modern Caiazzo; Renda, 2004, 354-356, site 365, figs. 96.13 and 17) and could be from *Allifae*. However, this form was also produced in the Bay of Naples as suggested by a carinated cup, judged to be of local production (Faga, 2008, 646, figure 3.13; 2010, 168, figure 2.2), which has similar dimensions and grooves at the *carina* and at mid-height of the wall but with a flat base without concentric grooves.

The deep hemispherical cup (Figure 2d-f) is similar to the Marabini XXXVI form (Marabini Moevs, 1973; cf. Mayet, 1975, form XXXIII, n. 272-274; Ricci, 1985, type 2/344). A peculiar feature of this cup is a thin moulding at mid-height or at two/thirds of the wall. As on the previous form, the wall may present a slight rouletting with vertical or oblique strokes limited to the upper part or the entire surface. The ratio between the diameters of the rim (between 8 and 12 cm) and the overall height of the vessel (about 1.2 / 1.4:1) seems relatively stable while the ratio between the diameter of the rim and that of the foot (1.9 / 2.5:1) is more variable. These cups were also produced in Naples (Faga, 2010b, 168, figure 2.8 e 17) and in *Etruria* (Faga 2010b, 170, 172, Figure 3.3), but they have one or more grooves on the wall and do not present the thin moulding that characterizes the vases from *Allifae*. No more than a generic comparison with the Marabini XXXVI form is also possible for the bowl (Figure 2g) which differs from the previous examples for the more elaborate rouletting on the body (for a similar vessel from the villa of San Rocco at Francolise [Ce] cf. Cotton and Metraux, 1985, 194, pl. 44.3).

Amongst the other TW vessels in the same fabric from the dump, there are a few fragments of a one-handled globular jug (Figure 2i), similar to the Marabini LI form (Marabini Moevs, 1973; Ricci, 1985, type 1/103) and a few cups similar to the Marabini XXXVI form, nn. 191-193 (Marabini Moevs, 1973). In the latter, the wall can

be plain (Figure 2h) or covered with rouletting; a good parallel for the plain version is offered by some pieces in a late first century B.C. deposit from *Herdoniae* (modern Ordona: De Boe and Vanderhoeven, 1979, 116-117, figure 27, nn. 41-42); similar is also an handled bowl fragment from the villa of San Rocco at Francolise (Ce; Cotton and Metraux 1985, 196, pl. 44.11).

The vessels of Figures 2k-l and Figure 2j, also in the same macroscopic aspect, were instead found in the excavation of a cooking ware pottery-kiln just outside "Porta Fiume". The first, similar to the Ricci beaker 1985, type 1/164 (cf. Mayet 1975, form XII, nn. 165-166), could form a "service" with the carinated cup (Figure 2a-c); several fragments of this form (the reconstruction of a complete profile was not possible), both with and without handles, occur in the dump of the Amodeo property. The vessels from *Allifae* could find a good parallel among the TW pottery from the cited Roman villa in the territory of *Caiatia* (Renda 2004, 354-356, site 365, figure 96.20) and in Naples (Faga, 2008, 646, figure 3.14-15). The shallow hemispherical bowl Figure 2j could be a variant of the Marabini XXXVI form (Marabini Moevs. 1973). A similar vessel, but without the groove that on the *Allifae* bowl runs along approximately 2/3 of the wall, was produced in the Bay of Naples (Faga, 2010b, figure 2.12; cf. the Kenrick bowl, 1985, 311, B455 from Benghazi, possibly of a Campanian source); a vessel from the cited Roman villa in the territory of *Caiatia* (Renda, 2004, 354-356, site 365, figure 96.10) could offer another parallel and could be from *Allifae*.

Twenty-one TW potsherds were selected for archaeometric investigations using mineralogical, textural and chemical analyses in an attempt to identify their main technological features such as firing temperatures, type of base clay and handling processes. The macroscopic aspect of the samples showed that the TW pottery is characterised by a very fine body

and its features likely suggest that the clayey deposits must have been handled, probably via a levigation process obtaining a fine-sized body. Moreover, the available data on clay raw materials from the Campania region infer the occurrence of a variable content of a coarse-sandy fraction in clays (De Bonis et al., 2013). With these assumptions, also the simple link "chemical composition to - provenance" could fail due to the fact that the removal of coarser grains can somehow affect the bulk chemical composition (De Bonis et al., 2013).

The archaeometric characterization of the potsherds can give an idea of the technical efforts necessary to produce such a peculiar ceramic product. Thus, this paper aims at deciphering the technology behind the TW pottery production also in terms of the clayey raw material used and the handcrafting process. Particular attention is devoted to what happens to a clayey material when the coarser fraction is removed. To this scope, clayey deposits (and their finer fraction) cropping out in the Alife area were compared from a chemical, mineralogical and textural point of view with the TW potsherds.

Finally, this paper aims at confirming a TW production in ancient Alife also by defining a reference group of TW pottery. The comparison with the available archaeometric data of other regional production will also highlight the framework of production sites and circulation of Campanian Thin Walled pottery.

Archaeometric overview of TW pottery from the Campania region

The TW pottery production spans from the II century BC to the II century AD, during the Republican and early Imperial flourishing periods of the Roman-Italic economy. The circulation and distribution of the TW pottery is an open discussion among archaeologists, who considered the transportation of these vessels difficult due to their brittleness. A regional production system with numerous centres of production in the western Mediterranean and a short-distance distribution is generally supported (Schindler Kaudelka, 2012). However the possibility of a long-distance circulation has also been documented (e.g., the Cala Culip IV shipwreck containing TW pottery among over 4000 fine-ware vessels; Millet, 1993).

The TW pottery is widespread in Roman archaeological contexts of the Campania region and have been widely investigated; the large availability of archaeometric data enables to highlight differences among production sites in terms of typology, technology and raw materials. TW pottery has been reported among other contemporary ceramic classes in several sites of the so-called "Bay of Naples".

The archaeological survey in the ancient city of Pompeii has always catalysed the interest of archaeologists and recently a TW kiln was discovered close to the city walls (Via dei Sepolcri, Cavassa et al., 2014), confirming a site of production in the Vesuvian area. Moreover, fragments of TW pottery from the "Casa di Bacco" in Pompeii and the deposits of Herculaneum have been characterized (Giannossa et al., 2012).

The analyses carried out on potsherds from Pompeii and Herculaneum highlighted some interesting problems regarding local productions and the provenance of the raw materials. The occurrence of a fine-grained/high CaO typology and a coarse-grained/low CaO production is attributed to a local manufacture with two different recipes, despite the lack of clear comparisons with production indicators (Mangone, 2011). The typological and visual examination of unfired and deformed vessels from the kiln in Pompeii seems to confirm the utilization of coarse-grained base clay with abundant and selected volcanic sand (Cavassa et al., 2014).

The archaeological patrimony of the city of Naples has been greatly enhanced by subway

excavation works. During the excavation work of the harbour, the old seafloor surface returned huge amounts of pottery that are useful for a more detailed reconstruction of the life and exchanges that occurred in the Roman port (Faga, 2008, 2010a, 2010b). Fragments of TW pottery are widespread inside these layers dating back to the end of III century AD - up to the beginning of V century (Faga, 2010a).

Archaeometric analyses (Faga, 2010b) highlighted the presence of both locally produced and imported vessels (Ager Falernus and Etruria). The potsherds are variable in chemical as well as mineralogical composition. As in the case of Pompeii (Mangone, 2011), a double manufacturing technology (fine-grained/high CaO vs. coarse-grained/low CaO) is reported attaining to a different choice of the raw materials.

Finally, the city of Cuma also represents an important site for ceramic production (Grifa et al., 2009; Morra et al., 2013), in two Roman contexts dated I century AD. It is worth noting the occurrence of kiln wastes and production indicators such as a stamp of a beaker (Cavassa, personal communication). The TW samples from Cuma are composed of quartz, white mica and subordinate brown mica. The other grains are quartz, feldspars (alkali feldspar and plagioclase), clinopyroxene, opaque oxides and brown mica as single crystals, associated with volcanic fragments. Pumices, obsidians, polycrystalline aggregates of quartz, ARF and calcite are scarce (Cavassa et al., 2012).

Geological setting

The town of Alife is located in a sector of the mid Volturno Valley, better known as the Alife plain (Figure 1). The plain was filled in the Quaternary by alluvial/lacustrine sediments, mostly represented by sandy clay and silt, often containing volcanics (pumices and lapilli) (Scarsella et al., 1971).

The northern sector of the plain is bordered

by the Matese mountains (southern Apennine chain), which reach a height of 2050 m above sea level and where alluvial fans developed at their foothills in the Quaternary. The Monti Trebulani massif that reaches a height of 1036 m above sea level borders the southern sector of the plain. The Matese and Monti Trebulani are formed by a carbonate platform succession (*Matese-Mt. Maggiore-Mt. Camposauro* unit; Bonardi et al., 2009), characterised by Mesozoic dolomite and dolomitic limestones (Trias-Lias). A disconformity marks the transition to Miocene deposits up to the clays with interbedded arenaceous turbidites of *Pietraroja* formation (Middle-Upper Tortonian). The clayey deposits of the *Pietraroja* formation also characterise some of the hills located in the eastern/south-eastern part of the plain; other hills are formed by the thrust-top sandstone formation of the *Arenarie di Caiazzo* (Lower Messinian).

Pyroclastic deposits are widespread in the Roccamonfina volcano area located west of the Alife plain. Ignimbrite deposits, ascribed to both the Roccamonfina and Campi Flegrei activity, can also be found in the depressions and at the mountain foothills in the southern sector of the plain.

Materials and Methods

Twenty-one fragments of TW pottery were collected; in addition, two raw clays were analysed and compared to the ceramic samples (Table 1). They were selected based on their chemistry and mineralogy among the carbonate-free clays outcropping in Northern Campania (detail about sampling strategy in De Bonis et al., 2013). The mineralogical and chemical features of the < 2μm fraction was also reported in order to enhance compositional changes induced by levigation processes (De Bonis et al., 2013).

Ceramic samples were analysed via Polarized Light Microscopy (PLM) evidencing the textural

Table 1. List of analysed ceramic fragments and clayey raw materials. Archaeological information and analytical techniques are showed.

	Sample	Form	PLM	XRPD	XRF	SEM/EDS
	GCA 1	Fig. 2.d-f	x	x	x	x
	GCA 2	wall sherd		x	x	
	GCA 3	Fig. 2.d-f	x	x	x	
	GCA 4	wall sherd	x		x	x
	GCA 5	base	x	x	x	
	GCA 6	Fig. 2.i		x	x	
	GCA 7	base	x	x	x	x
	GCA 8	Fig. 2.a-c	x	x	x	
	GCA 9	wall sherd		x	x	
	GCA 10	Fig. 2.g	x	x	x	
TW pottery	GCA 11	Fig. 2.a-c	x	x	x	x
	GCA 12	wall sherd	x	x	x	
	GCA 13	wall sherd	x		x	
	GCA 14	wall sherd	x	x	x	
	GCA 15	wall sherd	x	x	x	
	GCA 16	wall sherd	x	x	x	
	GCA 17	wall sherd	x		x	
	GCA 18	wall sherd	x	x	x	
	GCA 19	wall sherd	x		x	
	GCA 20	wall sherd	x	x	x	x
	GCA 21	wall sherd	x	x	x	
Clays	PMV2		x	x	x	x
	CSC1		x	x	x	x

Abbreviation: (PLM = Polarised Light Microscopy; XRPD = X-Ray Powder Diffraction; XRF = X-Ray Fluorescence; SEM/EDS = Scanning Electron Microscope/Energy-Dispersive X-Ray Spectroscopy).

and mineralogical features of the ceramic pastes. Microtextural and microstructural observations were carried out on ceramic representative samples (Table 1) using SEM images of a polished thin section obtained on a JEOL JSM-5310 electron microscope at the C.I.S.A.G. (Centro Interdipartimentale Strumentazioni per Analisi Geomineralogiche), University of Napoli Federico II). Grain Size and Pore Distribution (GSD and PSD) of the ceramic samples were performed on SEM images using ImageJ freeware software (ImageJ 1.44p, National Institutes of Health, USA; MultiSpec 3.1, Purdue Research Foundation). The GSD of the clayey sediment was carried out on a PLM micrograph from a thin section due to the coarser size of the grains. The grain and pores minimum Feret (mF) was measured in order to calculate the *phi* (Φ) values (Φ = -$\log_2$ (mF)) for the GSD and PSD evaluation. The *logit* of circularity (C; where *logit* = ln (C/1-C)) expresses the shape of the grains (Grifa et al., 2013).

Microchemical analyses on minerals of ceramics and clayey deposits have been performed at CISAG University of Napoli Federico II, by energy-dispersive spectrometry (EDS), using a Oxford Instruments Microanalysis Unit, equipped with an INCA X-act detector on a JEOL JSM–5310 microscope operating at 15 kV primary beam voltage, 50-100 mA filament current, a 15-17 mm spot size and a net acquisition-time of 50 s. Details of standards are provided in Melluso et al. (2010); relative analytical uncertainty is ~ 1% for major elements and 3-5% for minor elements.

X-Ray Powder Diffraction (XRPD) semi-quantitative analyses of potsherds and clayey deposits were carried out with a Philips PW1730/3710 diffractometer using the following operative conditions: CuKa radiation, incident and diffracted-beam Soller slits, curved graphite monochromator, 40 kV, 30mA, 3-70° scanning interval, step size = 0.02° 2θ and a counting time of 5s per step. Powders with a grain size < 10 mm were obtained using a McCrone microniser mill.

The bulk chemical composition of the ceramics, clayey deposits and their < 2μm fraction was obtained via X-Ray Fluorescence Spectrometry (XRFS) and major and trace elements were analysed with a Philips PW1400 spectrometer. The outer surfaces were abraded in order to avoid contaminated parts; the samples were milled in agate mortar in order to obtain pressed powder pellets. The detection limits and standard calibrations are reported in Melluso et al. (2005). The statistical procedures of chemical data were carried out using R freeware software (R Development Team, 2005).

Results and Discussions

Mineralogy and Textures of the TW samples

XRPD and PLM analyses (Table 2 and 3) revealed the ubiquitous presence of abundant quartz representing the main minerals of non-plastic inclusions (Figure 3a). Feldspars, both plagioclase (from labradorite to albite) and alkali-feldspar (orthoclase/sanidine) were present (Figure 4a; Supplementary Table 4a, downloadable on the journal site). Traces of clinopyroxene were also noticed (Figure 3b). They are uncoloured tiny crystals showing a diopsidic composition via SEM-EDS analyses (Supplementary Table 4a; Figure 4b); their composition is consistent with the clinopyroxene of the Roccamonfina volcano and other Plio-Quaternary volcanic complexes of the Tyrrhenian border (Conticelli et al., 2010).

Among non-plastic inclusions, lithic grains were found; they are volcanics (feldspar and clinopyroxene) and sandstone fragments (quartz and feldspars) (Figure 3c). The occurrence of both volcanic and sedimentary inclusions accounts for a mixed source of grains in the base clayey raw material.

Accessory phases (Supplementary Table 4b) mainly of a detrital origin, are garnet with a composition ranging from pyrope to almandine end-members (Locock, 2008). (Ce)-monazite

Table 2. XRPD semi-quantitative data of Alife TW pottery and clayey sediments.

	Qz	Fsp	Ilt	Cal	Hem	Hc	Mgh	Clay Minerals
GCA1	xxx	x			tr	tr	tr	
GCA2	xxxx	x				tr		
GCA3	xxxx	x	tr		tr			
GCA5	xxxx	x			tr	tr	tr	
GCA6	xxxx	x	xx	tr				
GCA7	xxx	x	tr		tr	tr	tr	
GCA8	xxx	x			tr	tr	tr	
GCA9	xxxx	x	tr		tr			
GCA10	xxxx	x	tr			tr	tr	
GCA11	xxx	x	tr			tr	tr	
GCA12	xxx	tr	tr			tr	tr	
GCA14	xxx	x			tr	tr	tr	
GCA15	xxxx	tr	tr				tr	
GCA16	xxxx	x	xx					Chl
GCA18	xxx	x	tr		tr	tr	tr	
GCA20	xxxx	tr	tr		tr			
GCA21	xxx	x	tr		tr			
PMV2	xxxx	xx	x		tr			IS Ilt/Sme; Kln
CSC1	x	xxx	xx	x		tr		Hal

Legend: xxxx = very abundant; xxx = abundant; xx = frequent; x = scarce; tr = trace.
Abbreviations (after Whitney and Evans. 2010): Qz = quartz; Fsp = feldspars (plagioclase and alkaline feldspar); Cal = calcite; Hem = hematite; Hc = hercynite; Mgh = maghemite; Chl = chlorite; IS Ilt/Sme = smectite mixed layers; Kln = kaolinite; Hal = halloysite.

Table 3. PLM observations and quantitative GSD data of analysed samples. For Alife TW pottery the PSD is also reported.

Sample	Matrix		Texture	Packing	Porosity	Grain size
	Colour	Activity				
GCA 1	light/dark brown	isotropic	serial	**15.71**	**9.29**	fine-coarse silt
GCA 3	red-orange	isotropic	serial	10-15%	L	fine-coarse silt
GCA 4	light brown	anisotropic	serial	**29.51**	**11.57**	medium-coarse silt
GCA 5	grey/brown	isotropic	serial	10-15%	L	fine-coarse silt
GCA 7	grey/red	isotropic	serial	**16.43**	**5.42**	fine-coarse silt
GCA 8	grey/brown	isotropic	serial	10-15%	L	fine-coarse silt
GCA 10	grey/brown	isotropic	serial	15-20%	L	fine-coarse silt
GCA 11	grey/brown	isotropic	serial	**15.32**	**10.5**	fine-coarse silt
GCA 12	grey/red	isotropic	serial	10-15%	L	fine-coarse silt
GCA 13	light brown	isotropic	serial	10-15%	L	fine-coarse silt
GCA 14	grey/red	isotropic	serial	10-15%	L	fine-coarse silt
GCA 15	grey/red	isotropic	serial	10-15%	L	fine-coarse silt
GCA 16	light brown	anisotropic	serial	10-15%	L	fine-coarse silt
GCA 17	red-orange	anisotropic	serial	10-15%	L	fine-coarse silt
GCA 18	grey/brown	isotropic	serial	10-15%	L	fine-coarse silt
GCA 19	grey	isotropic	serial	10-15%	L	fine-coarse silt
GCA 20	red-orange	isotropic	serial	**20.12**	**4.43**	medium-coarse silt
GCA 21	light/dark brown	isotropic	serial	10-15%	G	fine-coarse silt
PMV2	light brown		bimodal	15-20%		medium sand-fine silt
CSC1	dark reddish brown		bimodal	10-15%		coarse sand-medium silt

Abbreviations (after Whitney and Evans, 2010): Qz = quartz; Fsp = feldspars (plagioclase and alkaline feldspar); Bt = Biotite; Ms = muscovite; Cpx = clinopyroxene; Opq = opaque minerals; Cb = carbonate mineral; Amp = amphibole. Bold numbers of Packing and Porosity values represent the results of quantitative DIA. For Porosity: L = Low, G = Good.

Table 3. Continued…

Sample	Qz	Fsp	Bt	Ms	Cpx	Litics	Opq	Cb	Amp	Notes
				Grains						
GCA 1	xxxx	xxx	xx	xx	tr	x*	x			*qz+bt sandstone; cover
GCA 3	xxxx	xx	xxx	xxx	tr		xx	x	x(?)	dark brown covering
GCA 4	xxxx	xx	x	xx	tr					
GCA 5	xxxx	xx	xx	x						
GCA 7	xxxx	xx	xx	xx	x	x*				scoriae
GCA 8	xxxx	xx	xx	xx		x	xx			
GCA 10	xxxx	xx	xx	xxxx		tr	x			cover and alteration
GCA 11	xxxx	xx	x	xxx		tr*	x			scoriae; *qz+bt lithics
GCA 12	xxxx	xx	x	xxx	tr	tr		x		
GCA 13	xxxx	xx	x	xx	tr		x	xx		cover
GCA 14	xxxx	x	xx	x	x	x*	x	x		*Fsp+cpx volcanics
GCA 15	xxxx	xx	x	xx	tr		x			
GCA 16	xxxx	xx	x	xx			x			
GCA 17	xxxx	xx	xxx	xx	x			x		cover
GCA 18	xxxx	xx	x	xx				x		cover
GCA 19	xxxx	xx	x	xx	tr		x	x		cover
GCA 20	xxxx				tr	x*				scoriae; *qz+bt lithics
GCA 21	xxx	xxx	xx	xxx	tr		x			cover
PMV2	xxx	xxx	tr		xx	x				garnet; scoriae
CSC1		xxxx			x	tr	tr			scoriae; olivine

Abbreviations (after Whitney and Evans, 2010): Qz = quartz; Fsp = feldspars (plagioclase and alkaline feldspar); Bt = Biotite; Ms = muscovite; Cpx = clinopyroxene; Opq = opaque minerals; Cb = carbonate mineral; Amp = amphibole. Bold numbers of Packing and Porosity values represent the results of quantitative DIA. For Porosity: L = Low, G = Good.

also occurs showing La_2O_3 in the range 13.3-15.6 wt% and Ce_2O_3 from 28.2 to 31.6 wt%. Ti-rich magnetite occurs and TiO_2 ranges between 7.3 and 8.1 wt%. Rutile (TiO_2) was observed in GCA4 and 20. Zircon (ZrO_2) was analysed in GCA1 and 7 (1.6 -1.7 wt% HfO_2).

Microcrystalline secondary calcite has been observed inside the pores.

The non-plastic inclusions were scattered in a red/brown clay body often showing sharp or shaded colour zoning (Table 3, Figure 3d). Taking into account the low thickness of the walls and the type of sandwich structures, the colour zoning can be related to a change in the firing atmosphere rather than a short soaking time (Nodari et al., 2007). Sometimes a red/brown coating covered the walls; it is made of a fine clayey material on average 1 mm thick.

From a textural point of view, all the examined samples have a very fine GSD (Figure 5) and a packing varying from 15 to 30% (Table 3).

The GSD varies from fine to coarse silt ($7 < \Phi < 4$; 0.008 to 0.062 mm), with the exception of the samples GCA4 and 20 that show slightly coarser grains (medium - coarse silt; $6 < \Phi < 4$; 0.016 to 0.062 mm). The serial texture of the samples is supported by the shape of the GSD and by the similar values of mean and median (Table 5). Standard deviation of the Φ values indicates a moderate sorting of grains (0.75 - 1.00 $\sigma(\Phi)$; Table 5). The *logit* curves and related statistical parameters (Table 5) indicate a main circular shape for the majority of the grains (Figure 5).

The PSD of the TW pottery evidences that as
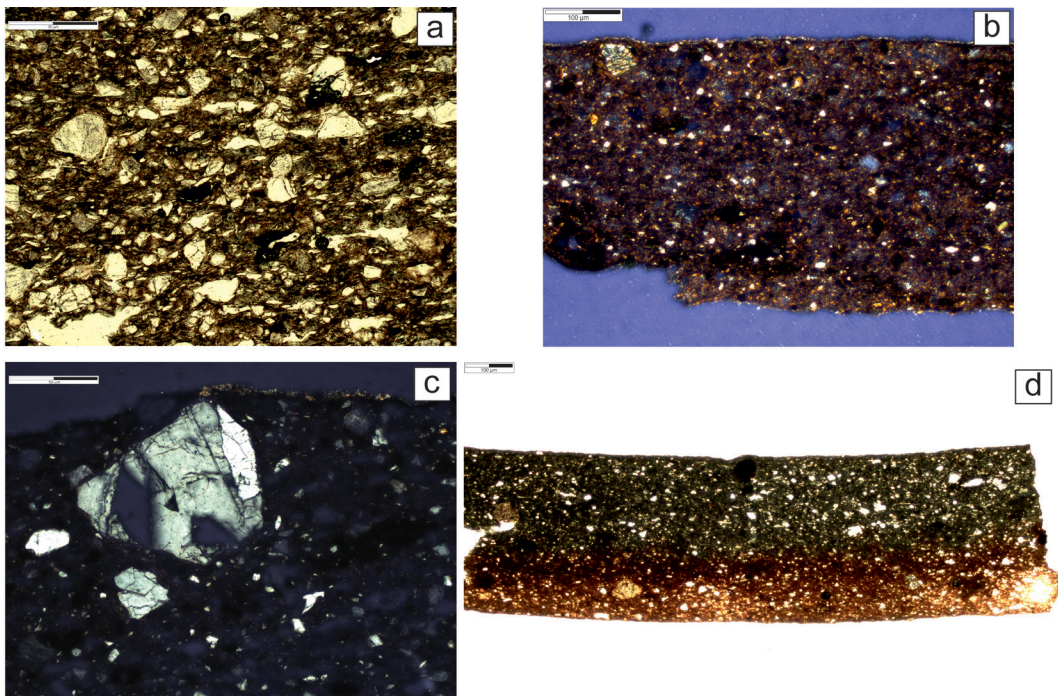
Figure 3. Representative microphotographs of TW analyzed samples; a) quartz and feldspars grains. GCA 4, plane polars; b) clinopyroxene crystal scattered in quartz-feldspar rich matrix. GCA 7, crossed polars; c) polycrystalline quartz grain. GCA 1, crossed polars; d) colour zoning of the body. GCA 18, plane polars.

the pore size decreases the pore shape tends to be more circular as showed by the mean and median values of pore size and pore circularity (Figure 5; Table 5).

The only exception is sample GCA 20 which also has the largest pore size and standard deviation values of circularity (1.19 and 1.38,

respectively, Table 5).

As far as micro and cryptocrystalline phases are concerned, XRD analyses (Table 2) allowed us to point out any firing process parameter such as temperatures and redox conditions. The newly-formed phases (during firing process) are mainly Fe-oxides. Hematite (Fe_2O_3) and/or
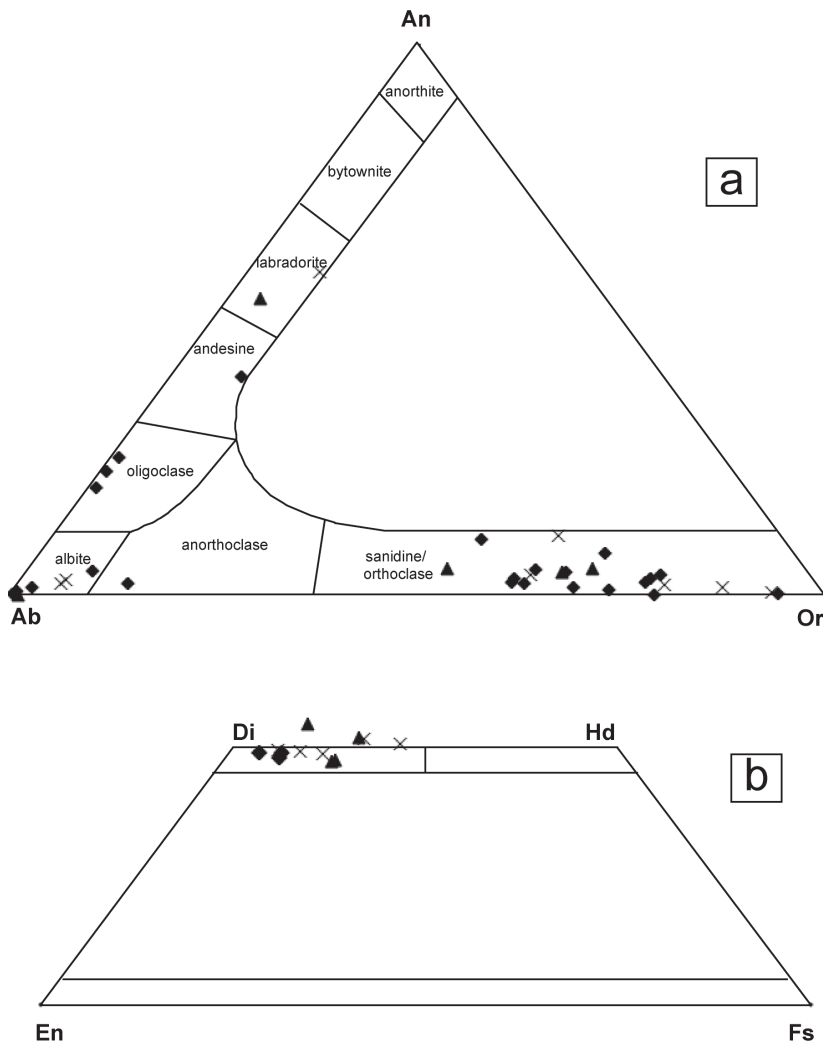
Figure 4. Chemical composition of feldspars; a) MacKenzie and Zussman (1974) and clinopyroxene; b) Morimoto (1988) of TW samples (diamond) and clayey deposits (triangle = PMV 2 and cross = CSC 1).
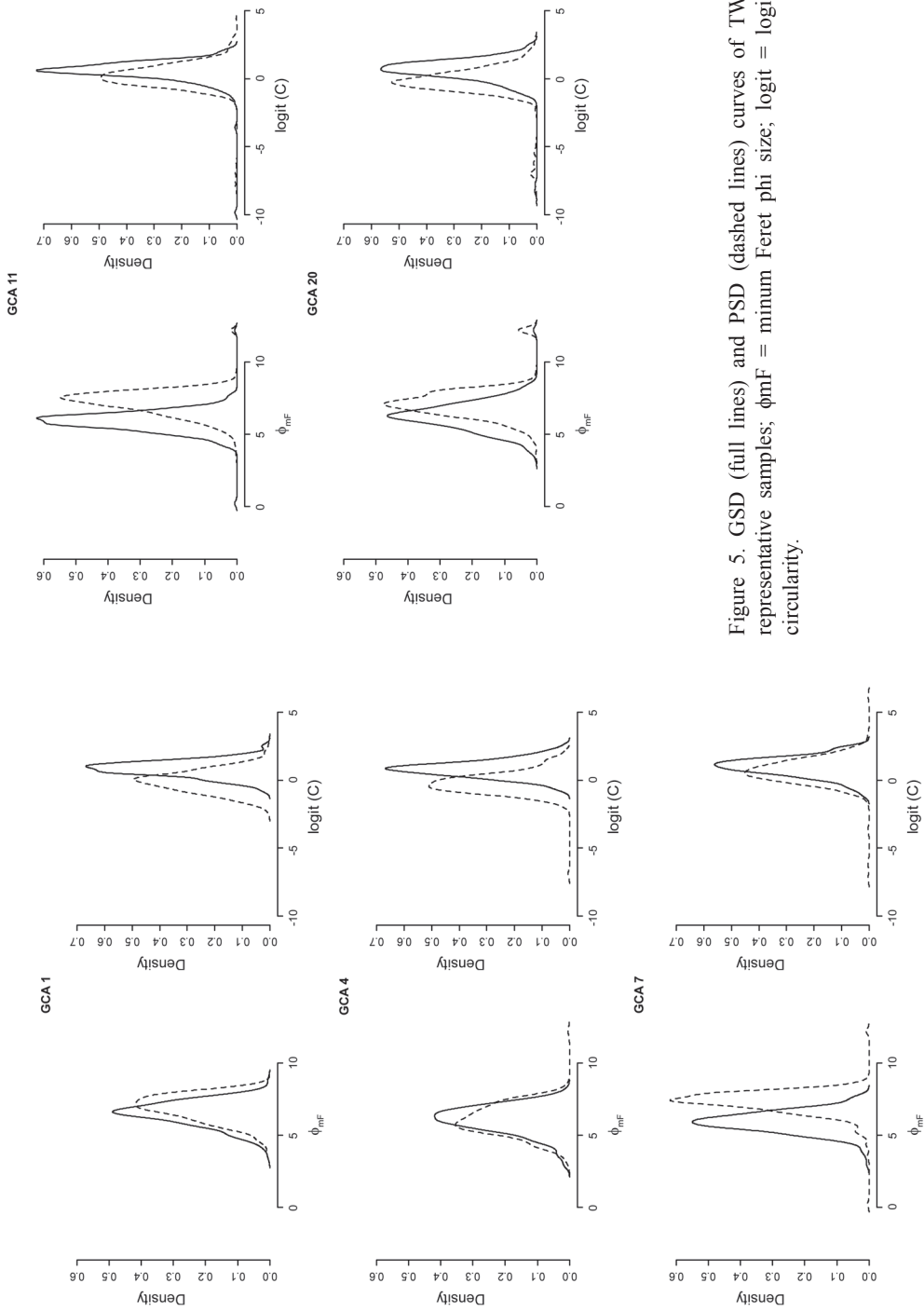
Figure 5. GSD (full lines) and PSD (dashed lines) curves of TW representative samples; φmF = minum Feret phi size; logit = logit circularity.

Table 5. Statistical parameters of the GSD of TW pottery and clayey deposits; PSD is also reported for the TW samples. t = standard deviation.

	GSD								PSD					
	Size		Logit Circularity				Size		Logit Circularity		
	σ(φ)	mean	median	σ(logit (C))	mean	median	σ(φ)	mean	median	σ(logit (C))	mean	median
GCA 1	0.87	6.46	6.54	0.60	0.84	0.87	0.92	6.88	6.99	0.81	-0.10	-0.09
GCA 4	0.97	6.06	6.13	0.63	0.83	0.82	1.08	6.05	6.04	0.86	-0.21	-0.24
GCA 7	0.76	5.92	5.94	0.73	0.99	1.03	0.86	7.29	7.39	1.00	0.64	0.65
GCA 11	0.79	5.90	5.93	0.87	0.57	0.64	0.92	7.19	7.30	1.06	0.20	0.21
GCA 20	1.03	6.26	6.27	1.00	0.62	0.71	1.19	7.20	7.12	1.38	-0.27	-0.19
CSC1	0.87	3.86	4.03	0.68	1.43	1.45						
PMV2	0.82	4.82	4.96	0.65	1.40	1.41						

hercynite ($Fe^{2+}Al_2O_4$) and/or maghemite (γ-Fe_2O_3) are present in all the samples with the exception of GCA 6 and GCA 16 (which account for the highest illite/mica content) (Table 2). In addition, it is worth noting the simultaneous occurrence of different Fe-bearing minerals in samples GCA1, 5, 7, 8, 10, 11, 12, 14 and 18 that also accounts for the grey/red-zoning colour of ceramic body due to reductive/oxidative changes during firing dynamics (Figure 3d) (Nodari et al., 2007; Morra et al., 2013). The fO_2 variation could have influenced the temperature of mineral reactions over the firing process thus the equivalent firing temperature estimation (Maggetti et al., 2011 and reference therein). Nevertheless, the firing temperatures were mainly inferred on the persistence of the illite-like phases detected as a hydroxilited phase up to about 950 °C (Cultrone et al., 2001).

If no illite-like phases occur (Table 2), the estimated firing temperatures can range between 950-1000 °C (the upper limit is consistent with the lack of mullite; Cultrone et al., 2001). Where only illite-like phases are present (Table 2), a temperature lower than 950 °C can be inferred (Cultrone et al., 2001).

Finally, sample GCA 6 was most likely fired at lower temperature (700-750 °C), due to the fact that chlorite was still barely noticeable (De Bonis et al., 2014; Nodari et al.. 2007). Sample GCA 16 accounts for a slightly higher T (750-800 °C) due to the presence of illite.

A relationship between pore system features (size and shape) and firing temperatures can be accounted. The size and shape of the pores, linked to the firing temperatures, account for a different stage of sintering among the samples. The illite/mica-bearing samples had slightly larger and more circular pores that became smaller and elongated due to the ongoing sintering process as the temperature increased (Cultrone et al., 2001).

Raw materials

The TW samples show a quite homogeneous chemical composition, attesting low-CaO (0.8 - 3.4 wt%) and high-SiO_2 concentrations (62.6-69.9 wt%, Figure 6; Table 6); the GCA2, 4 and 9 samples can be distinguished for their lower titanium, iron and magnesium content, as well as Ni and Cr (Table 6 and Figure 6). The same samples (GCA 2, 4 and 9) can be grouped together due to their high alkali content, along with sample GCA 11 that is marked by a higher K_2O content (4.9 wt%). Trace elements show a wider variability (Table 6) despite barium again distinguishes samples GCA2, 4 and 9; GCA 6 can be also distinguished for the highest Ba concentration (649 ppm, Table 6).

Starting from the chemical composition of the potsherds and assuming an almost isochemical firing process (Grifa et al., 2009), it is possible to suggest that the source of the clayey raw materials might be identified among the low-CaO clays of the Northern Campanian area. Based on this assumption, an alluvial and a weathered pyroclastic deposits cropping out in the area have been compared in order to identify the clay type used for TW manufacture (PMV2 and CSC1, De Bonis et al., 2013).

The clayey deposits were mostly composed of quartz, alkali feldspar (near-pure albite and orthoclase/sanidine) and plagioclase (labradorite) (Figure 4a). Feldspars were more abundant in CSC1 than in PMV2 (Figure 7a; Table 2).

A volcanic component was observed in both samples, and it is represented by loose crystals of diopsidic clinopyroxene (Figure 4b) and rare pumices and scoriae (sometimes leucite-bearing) with a trachytic and trachy-phonolitic composition (Figure 7b; Table 3). Traces of volcanic garnet were present in the PMV2 samples (Figure 7c; andradite 61.5 mol% – grossular 19.9 mol%; Locock, 2008) along with phlogopite, amphibole, Ti-rich magnetite, apatite, dolomite, calcite and arenitic grains (Figure 7d; Table 3).

Clay minerals were represented by illite, an illite/smectite mixed layer (I/S) and kaolinite. The CSC1 accounts for the occurrence of halloysite (Table 2).
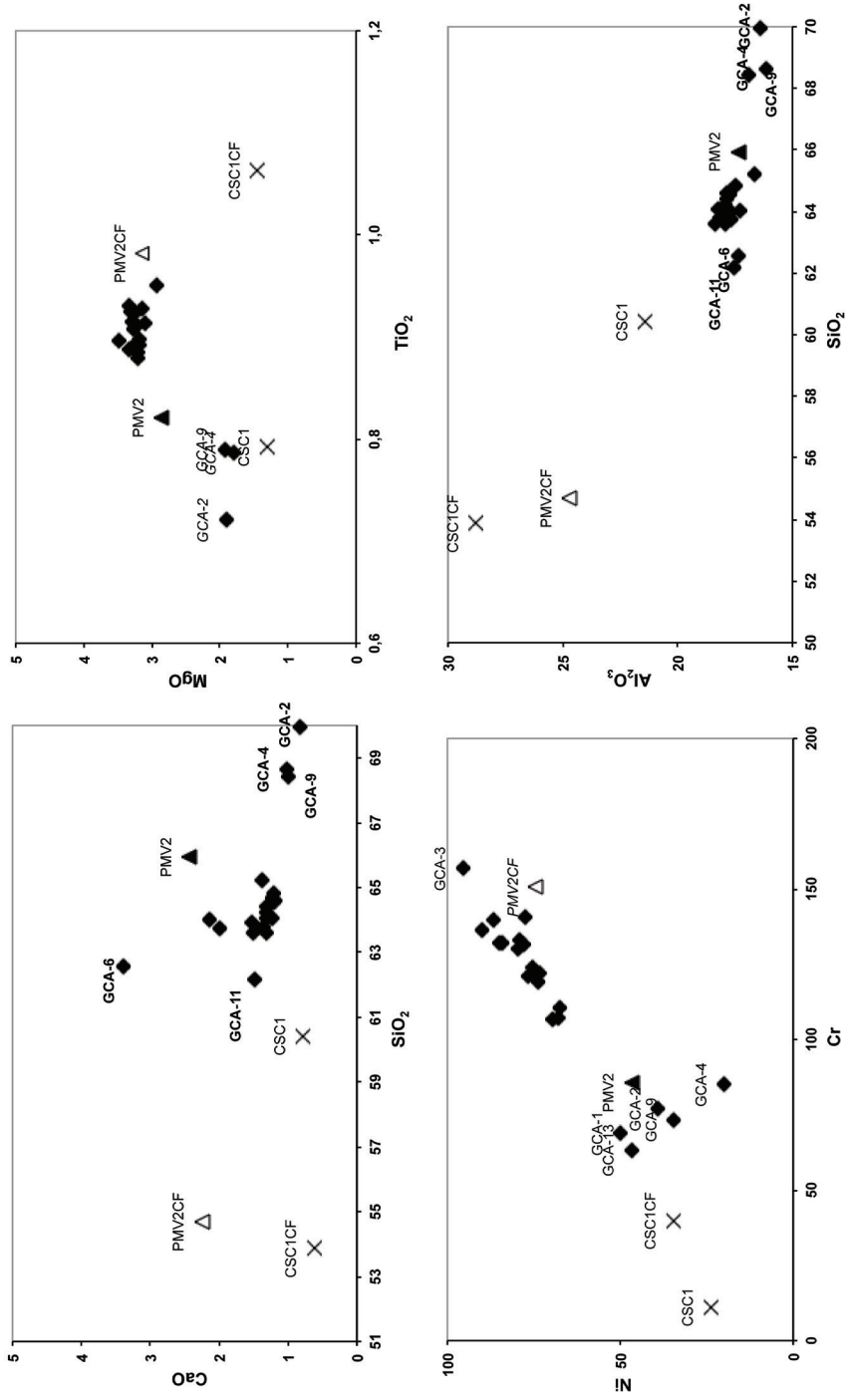
Figure 6. Selected major and trace elements diagrams of Alife TW pottery (diamonds) and clayey sediments (triangle = PMV 2 and cross = CSC 1).

Table 6. XRF data of the TW pottery and clayey sediments (major elements are in %wt of oxides, traces elements in ppm). The clay fraction of PMV2 and CSC1 is also reported (PMV2CF and CSC1CF).

	SiO$_2$	TiO$_2$	Al$_2$O$_3$	Fe$_2$O$_3$	MnO	MgO	CaO	Na$_2$O	K$_2$O	P$_2$O$_5$	Tot	LOI
GCA 1	65.22	0.95	16.67	7.96	0.19	2.93	1.37	0.99	3.57	0.15	100	3.45
GCA 2	69.94	0.72	16.40	5.65	0.04	1.91	0.82	1.23	3.25	0.03	100	
GCA 3	64.67	0.89	17.70	7.94	0.16	3.18	1.24	1.00	3.08	0.15	100	
GCA 4	68.65	0.79	16.17	5.99	0.07	1.80	1.02	1.32	4.16	0.05	100	
GCA 5	64.42	0.89	17.89	7.90	0.16	3.29	1.31	0.95	3.05	0.14	100	2.27
GCA 6	62.58	0.90	17.38	7.05	0.09	3.48	3.40	0.73	3.29	1.12	100	3.91
GCA 7	64.07	0.89	18.21	7.92	0.16	3.32	1.23	0.94	3.10	0.15	100	
GCA 8	64.54	0.90	17.73	7.92	0.16	3.17	1.21	0.98	3.25	0.13	100	4.21
GCA 9	68.42	0.79	16.92	6.01	0.06	1.92	1.00	1.17	3.59	0.12	100	1.54
GCA 10	63.93	0.91	17.75	7.99	0.16	3.27	1.53	0.95	3.29	0.22	100	
GCA 11	62.16	0.93	17.51	8.37	0.17	3.32	1.47	0.84	4.96	0.26	100	2.38
GCA 12	63.77	0.91	18.07	8.07	0.17	3.28	1.37	0.90	3.28	0.17	100	
GCA 13	64.03	0.88	17.26	7.29	0.14	3.20	2.14	0.69	3.50	0.87	100	
GCA 14	64.07	0.93	17.82	8.07	0.17	3.14	1.32	0.93	3.40	0.15	100	4.45
GCA 15	63.61	0.92	17.94	8.18	0.18	3.24	1.50	0.89	3.33	0.20	100	1.93
GCA 16	63.75	0.88	17.66	7.57	0.15	3.20	1.98	0.70	3.32	0.80	100	
GCA 17	64.83	0.91	17.47	8.00	0.16	3.11	1.21	1.01	3.18	0.13	100	1.83
GCA 18	63.80	0.91	18.17	8.05	0.17	3.28	1.36	0.91	3.16	0.19	100	3.52
GCA 19	63.59	0.93	18.38	8.09	0.16	3.30	1.31	0.87	3.21	0.16	100	2.78
GCA 20	64.62	0.89	17.84	7.91	0.16	3.24	1.19	0.93	3.07	0.15	100	1.98
GCA 21	64.22	0.91	17.91	7.97	0.16	3.23	1.32	0.90	3.18	0.20	100	1.12
PMV2	65.94	0.82	17.37	6.18	0.23	2.86	2.43	0.87	3.19	0.11	100	11.74
CSC1	60.42	0.79	21.41	6.54	0.21	1.31	0.78	2.32	6.11	0.10	100	11.18
PMV2CF	54.69	0.98	24.71	10.57	0.25	3.14	2.25	0.30	3.00	0.11	100	
CSC1CF	53.87	1.06	28.77	7.97	0.21	1.44	0.62	1.60	4.29	0.15	100	

Table 6. Continued…

	Rb	Sr	Y	Zr	Nb	Ba	Cr	Ni	Sc	V
GCA 1	76	85	21	115	14	236	69	50	13	81
GCA 2	145	127	22	207	24	553	77	39	14	108
GCA 3	134	143	39	177	20	425	157	96	20	154
GCA 4	251	119	22	226	28	448	85	20	11	35
GCA 5	133	143	37	173	19	409	136	90	15	142
GCA 6	146	168	29	160	20	649	107	70	16	139
GCA 7	173	155	45	226	26	414	132	85	21	145
GCA 8	113	123	33	150	17	382	121	77	14	128
GCA 9	176	148	26	227	26	589	73	34	11	131
GCA 10	144	144	39	188	22	400	124	75	15	134
GCA 11	221	141	37	186	20	461	133	79	15	152
GCA 12	150	139	39	194	23	407	122	73	16	134
GCA 13	73	95	19	108	13	353	63	47	13	83
GCA 14	140	128	33	178	21	361	110	68	15	128
GCA 15	139	137	36	175	20	406	119	74	16	130
GCA 16	142	136	31	171	19	553	107	68	18	156
GCA 17	135	133	35	181	21	376	132	78	19	138
GCA 18	117	136	33	152	16	412	140	87	17	142
GCA 19	101	121	30	136	14	407	141	78	17	125
GCA 20	141	146	41	181	21	422	132	84	21	135
GCA 21	127	132	33	167	19	397	130	80	19	136
PMV2	173	241	35	242	27	653	86	47	13	127
CSC1	372	332	48	485	72	585	11	24	8	98
PMV2CF	230	165	46	245	42	626	150	74	21	186
CSC1CF	360	211	83	756	97	659	39	34	14	66
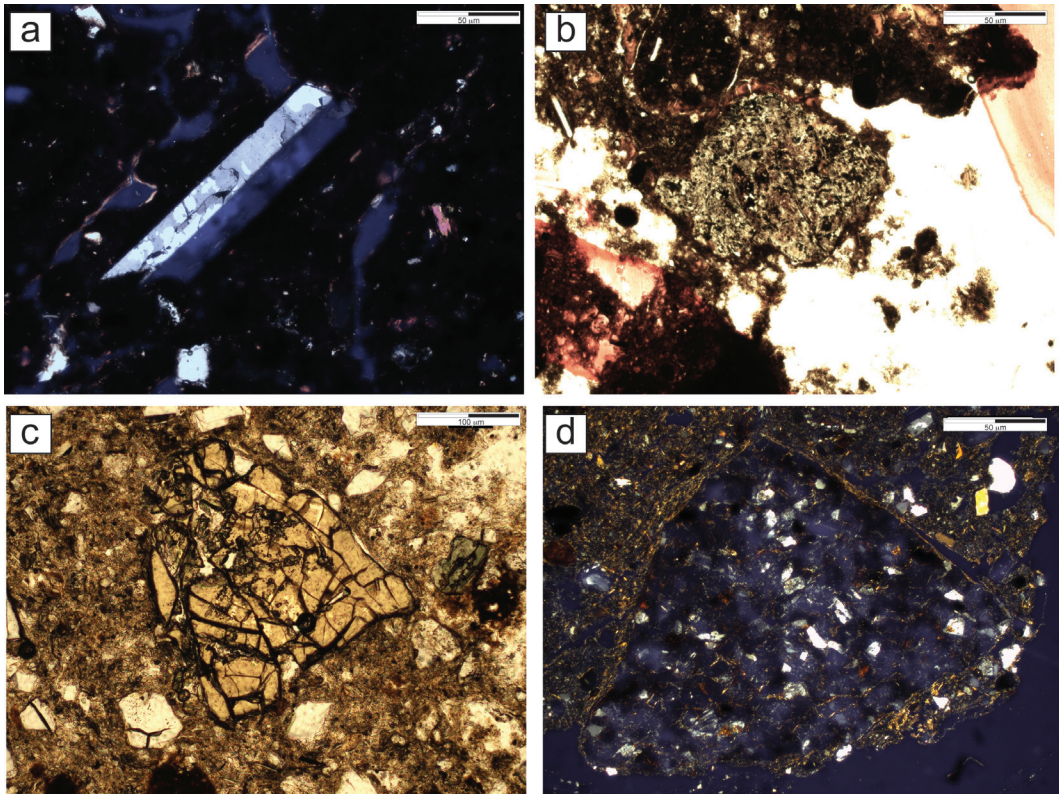
Figure 7. Representative microphotographs of clayey sediments; a) sanidine crystal, CSC 1, crossed polars; b) volcanic scoria, CSC 1, crossed polars; c) garnet and clinopyroxene crystals, PMV2, plane polars; d) arenitic grain, PMV 2, crossed polars.

CaO ranges from 0.8 (CSC1) up to 2.4 wt% (PMV2) and sample CSC1 accounts for the highest alkali content as well as Rb (372 ppm), Sr (332 ppm), Ba (585 ppm) and Zr (485 ppm) content, reflecting its volcanic origin (Table 6).

For some elements such as alkali, silica and calcium oxides, aluminium and magnesium, the composition of PMV2 closely resembles those of TW pottery, although some differences are present (Table 6; Figure 6). In fact. the main group of TW samples shows a higher Ti, Ni and Cr and lower Sr content than the PMV2 (Figure 6).

We investigated the possibility that these differences could be attributable to a levigation process employed to remove the coarser fraction (sandy grains) by settling in order to obtain a finer clay body. To this end we compared the GSD of clays and TW pottery.

GSD obtained by Image Analyses of the CSC1 shows a Φ size curve mainly comprised of medium silt/fine sand particle sizes ($2 < \Phi < 6$, mean value = 3.86, Table 5) and a subordinate coarse/very coarse sand (Φ size up to 1). as shown by the negative tail of curve (Figure 8). The standard deviation value ($\sigma(\Phi) = 0.87$) suggests a moderate sorted distribution of the inclusions. The circularity histogram (Figure 8) highlights the sub-circular shape of the particles
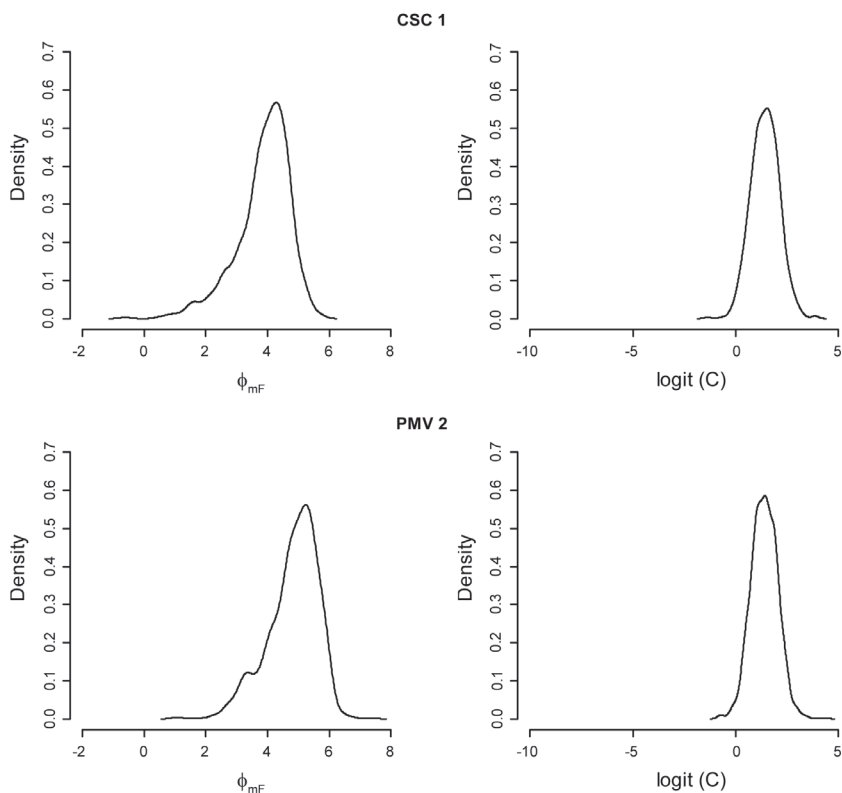
Figure 8. GSD curves of clayey sediments; ΦmF = minum Feret phi size; logit (C) = logit circularity.

as showed by standard deviation (0.6), mean and median values (1.4) (Table 5).

The PMV 2 has a finer grain size distribution that ranges from very fine silt (0.01 mm) to medium sand (0.50 mm); once again the histogram (Figure 8) shows a skewness toward coarser grains and a moderate sorting ($\sigma(\Phi)$ = 0.82) of the particles. The inclusions generally present a subcircular shape (average circularity = 0.78), with a small percentage of poorly elongated grains, as displayed by the negative tail of the PDF curve of the circularity histogram (Figure 8).

Comparing the GSD of clayey samples and

TW pottery, the Φ of clayey samples and TW samples deposits were higher than those of the clayey deposits. The GSD curves also infer the lack of the medium/fine to coarse/very coarse sand fraction thus supporting the hypothesis of the levigation of the base clay.

We then proceeded with the comparison of the chemical composition between the < 2μm fraction of the clayey deposits and the potsherds (Table 6; Figure 6). The effect of a levigation employed by the potters can be mostly verified in a SiO_2 depletion and Al_2O_3 enrichment due to the effects of the removal of quartz and feldspar and the consequent clay minerals accumulation. Other

Cluster Dendrogram
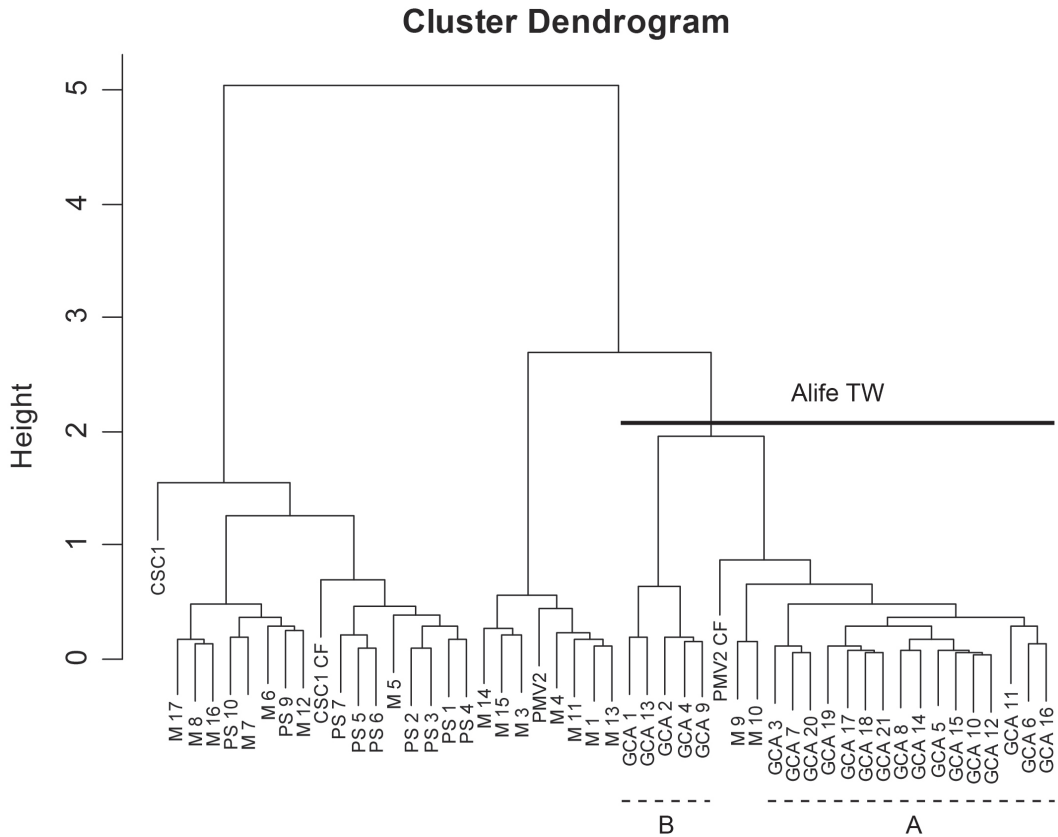
Figure 9. Hierarchical Cluster Analyses of TW pottery from Campania region; PS samples from Cuma (Cavassa et al., 2012); MNM samples from Napoli (Faga, 2010b).

secondary effects were noticed like Sr depletion and Ba and Rb enrichment following the same crystals removing/accumulation (Brouwer et al., 1983). The TiO_2 and Fe_2O_3 enrichment by coarse grain separation accounts for the phyllosilicates (micas) fractionation. The CaO does not vary significantly due to the fact that carbonates are almost absent.

Furthermore, the chemical diagrams of Figure 6 evidence that the main group of TW pots generally cluster between the PMV2 sample and its clay fraction, allowing us to infer the use of an alluvial-like deposit after coarser fraction

removal. Ni vs Cr diagram (Figure 6) also highlights some outliers such as GCA 2, 4 and 9 and GCA 1 and 13; the further differences have also been evidenced by multivariate analyses (see below).

Comparison with other TW regional productions

Chemical, mineralogical and textural features of TW from Alife have been compared with other production from the Campania region.

A first step has been a statistical approach on a dataset of chemical analyses of TW pottery from different sites, namely the TW pottery from the

Table 7. Weight of the variables of each Principal Component (Comp.)

	Comp.1	Comp.2	Comp.3	Comp.4	Comp.5	Comp.6	Comp.7	Comp.8	Comp.9
SiO_2		0.446	-0.23	0.261		-0.381	-0.15	-0.308	
TiO_2	0.114	-0.375	0.275		0.428	-0.583	-0.213		
Al_2O_3	-0.227	-0.306	0.309	0.17	0.141	0.159	0.11	-0.279	0.351
Fe_2O_3	0.218	-0.331	0.303			-0.154			-0.331
MgO	0.339				-0.28			0.21	
Na_2O	-0.297	0.12	-0.153			-0.543	0.125	0.447	0.218
K_2O	-0.244		0.351	-0.244	-0.589	-0.185	-0.362		
Rb	-0.284	-0.219	-0.161		-0.229		-0.385	-0.115	-0.381
Sr	-0.153	-0.26	-0.434	-0.501	0.12		0.192	0.193	-0.238
Y	-0.199	-0.299		0.552	-0.328		0.295		
Zr	-0.317	-0.191	-0.232	0.107	0.132				
Nb	-0.327	-0.164		0.108		0.134	-0.135		
Cr	0.265	-0.108	-0.321	0.338			-0.456		-0.141
Ni	0.319	-0.134		0.19	-0.289		0.371		-0.223
Sc	0.244	-0.266	-0.219			0.146	-0.348	0.425	0.516
V	0.196	-0.257	-0.326	-0.297	-0.289	-0.259	0.107	-0.577	0.383
Standard Deviation	2.735	1.859	1.273	0.931	0.749	0.664	0.633	0.584	0.505
Proportion of Variance	0.467	0.216	0.101	0.054	0.035	0.028	0.025	0.021	0.016
Cumulative Proportion	0.467	0.683	0.785	0.839	0.874	0.902	0.927	0.948	0.964

Roman port of *Neapolis* (Faga, 2008, 2010a, 2010b; Guarino et al., personal communication) and the TW samples from Cuma where a site of production has been suggested (Cavassa et al., 2012).

The statistical calculation were carried out on $\log_{10}$-transformation values of both major and trace elements data (all data set have been normalised to 100% ; moreover, some elements such as CaO, MnO, P_2O_5 and Ba were not considered as they could have been affected by post-earthen contamination (Maggetti, 1992; Cultrone et al., 2010; Grifa et al., 2009 and reference therein).

In order to further reduce the original dataset a Principal Component Analysis (PCA) was carried out resulting a 96% of total variance at the 9th Component (Table 7); the variables that mostly affect the first nine components are: SiO_2, TiO_2, MgO, Na_2O, K_2O, Sr, Y, Cr and Sc. These elements were used to perform a Hierarchical Cluster Analyses (HCA) using a Ward's linkage method (Figure 9).

HCA permitted to clearly distinguish the Alife potsherds from other regional productions from Cuma and Naples (cut at about 2.0 height, Figure 9); moreover, the Alife TW form two subgroups: subgroup A composed by the majority of local vessels along with some exotic samples (M9 and 10) likely belonging to Tuscanian production (Faga, 2010; Guarino et al., work in progress) and the finer fraction of PMV2 clayey sample. The subgroup B is composed by the outliers GCA 1, 2, 4, 9 and 13 to which a local manufacture can also be assigned, probably using a slight different raw materials as well as a different handing process.

Despite these slight differences also the statistical procedures also allowed to confirm the occurrence of a reference group of TW pottery from Alife.

It was impossible to carry out a similar chemical comparison with the production from Pompeii/Herculanum reported in Mangone

(2011) since available literature data refer to in situ analyses of the sole clay matrix, ignoring the contribution of coarser grains. However, the potsherds from Alife can be distinguished from those of Vesuvian production by the different texture and different abundance of volcanic grains observed in group 1 of Giannossa et al. (2012), and by the use of a high-CaO base clay in group 2 (Giannossa et al., 2012).

Conclusions

The archaeometric characterisation of the Thin Walled pottery from Alife highlighted a refined technology behind such a ceramic class in terms of raw materials, handling and firing processes.

The ancient potters probably exploited a low-CaO alluvial clayey deposit from the Middle Valley of the Volturno River. The sediment was then handled by a levigation process in order to remove the coarser grains. The result of the levigation process was a more plastic raw material, thus improving workability necessary to produce such thin walls.

The firing treatment was high (up to 950 °C), but the atmosphere changed during firing; this is evident by the grey/red-brown colour zoning of the pastes and the occurrence of different Fe-oxides and hydroxyls. This feature could be considered accidental (wrong firing) or intentional (fast firing) since the ancient potters could save and preserve the aesthetic features of the vessels using a thin coating. The archaeological data seems to support the first hypothesis as the fragments were found in a big TW dump.

The archaeological and archaeometric data allowed to confirm a local production and the circulation network of TW in Campania region will be more precisely defined when archaeometric data from the well-established or mostly-unknown key-sites of production, such as Pompeii and Cales will be available.

However, in the case of the *Allifae* production.,the comparison could be extended

beyond the Campania region. In fact, if one considers only the shapes of the TW from *Allifae*; they are characterized by a formal repertoire that, although close to that of other regional and extra-regional production centre, presents peculiar elements (e.g.: articulation of the bases of carinated and deep hemisferical cups, thin moulding on the wall of the latter). At that time, it would have been confined to the middle Volturno valley, although a regional or extra-regional distribution cannot be excluded. To this regard, it is useful to remember the verses of Horace (*Sermones*. II. 8. 39: *invertunt Allifanis vinaria tota*) where the A*llifana* are mentioned. The scholiasts on Horace explain *Allifana* as deep beakers or cups used as tableware (Porph., *ad l.*; Ps. Acr., *ad l.*). Indeed, according to one of the *scholia* collected by Pseudo- Acro, *Allifana* would have been *fictiles et subtiles*, that is to say a kind of pottery characterized by very thin walls. This leads us to exclude the hypothesis formulated by Salmon (1967, 000) that *Allifana* were "*rough paste pottery*" while it would be reasonable to link the *Allifana* with "thin walled" pottery. If so, Horace's verse would demonstrate the importation of these products in Rome in the third quarter of the first century BC and the fame of *Allifana* on the urban market.

Acknowledgements

References

Bonardi G., Ciarcia S., Di Nocera S., Matano F., Sgrosso I. and Torre M. (2009) - Carta delle principali Unità Cinematiche dell'Appennino meridionale. *Italian Journal of Geosciences*, 128 (1), 47-60.

Brouwer E., Baeyens B., Maes A., Cremers A. (1983) - Cesium and rubidium ion equilibriums in illite clay - *Journal of Physical Chemistry* 87(7), pp 1213-1219.

Cavassa L., Lemaire B. and John-Marc Piffeteau, (2014) - *Pompéi. L'atelier de potier* , *Chronique des activités archéologiques de l'École française de Rome* (on line). URL: http://cefr.revues.org/881

Conticelli S., Laurenzi M.A., Giordano G., Mattei M., Avanzinelli R., Melluso L., Tommasini S., Boari E., Cifelli F. and Perini G. (2010) - Leucite-bearing (kamafugitic/leucititic) and -free (lamproitic) ultrapotassic rocks and associated shoshonites from Italy: constraints on petrogenesis and geodynamics. In: The Geology of Italy: tectonics and life along plate margins. (eds): M. Beltrando. A. Peccerillo. M. Mattei. S. Conticelli and C. Doglioni. *Journal of the Virtual Explorer*, Electronic Edition, volume 36, paper 20.

Cotton M.A., Metraux G. P. R. (1985) - The San Rocco villa at Francolise. London, 282 p.

Cultrone G., Rodríguez-Navarro C., Sebastián E., Cazalla O. and de la Torre M.J. (2001) - Carbonate and silicate phase reactions during ceramic firing. *European Journal of Mineralogy*, 13, 621-634.

De Boe G. and Vanderhoeven M. (1979) - Un lot de céramique du troisieme quart du Ier siècle avant J.-C. In: Ordona VI**.** Rapports et Études. (ed.): J. Mertens, Bruxelles - Rome 1979, 107-127.

De Bonis A., Grifa C., Cultrone G., De Vita P., Langella A. and Morra V. (2013) - Raw materials for archaeological pottery from the Campania region of Italy: a petrophysical characterization. *Geoarchaeology,* 28 (5), 478-503.

Faga I. (2008) - Ceramica a pareti sottili nella Campania romana tra età tardo-repubblicana e prima età imperiale. Nuovi dati dal porto di *Neapolis*. SFECAG. Actes du Congrès de L'Escala-Empúries. 643-654.

Faga I. (2010a) - Ceramica «a pareti sottili» della prima

età imperiale dal porto di Neapolis. Primi risultati dello studio crono-tipologico. RCRF. 189-198.

Faga I. (2010b) - Vasi a pareti sottili dal porto di Neapolis: tecnologia e archeometria. *Rivista di Archeologia*, 34, 159-176.

Giannossa L.C., De Benedetto G.E., Laviano R., Pallara M., Mangone A. (2012) - Archaeometry in the Vesuvian Area: Technological Features of Thin-Walled Ware. *Proceedings of the 39th International Symposium for Archaeometry "50 years of ISA"*, Leuven (28 May-1 June 2012).

Grifa C., Cultrone G., Langella A., Mercurio M., De Bonis A., Sebastián E. and Morra V. (2009) - Ceramic replicas of archaeological artefacts in Benevento area (Italy): petrophysical changes induced by different proportions of clays and temper. *Applied Clay Science*, 46 (3), 231-240.

Grifa C., De Bonis A., Langella A., Mercurio M., Soricelli G. and Morra V. (2013) - A Late Roman ceramic production from Pompeii. *Journal of Archaeological Science*, 40,810-826.

Kenrick Ph. (1985) - Excavation at Sidi Khrebish Benghazi (Berenice). Volume III. 1: The Fine Pottery. *Supplements to Libya Antiqua*, 5, Tripoli.

Locock A.J. (2008) - An Excel spreadsheet to recast analyses of garnet into end-member components, and a synopsis of the crystal chemistry of natural silicate garnets. *Computers and Geosciences*, 34, 1769-1780.

Mangone A. (2011) - Ceramica a pareti sottili da Pompei ed Ercolano. Provenienza e tecnologia di produzione da un'indagine chimico-fisica. *Quaderni dell'"Orazio Flacco"*,1, 147-158

Maggetti M., Neururer Ch. and Ramseyer D. (2011) - Temperature evolution inside a pot during experimental surface (bonfire) firing. *Applied Clay Science*, 53, 500-508.

Marabini Moevs M.T. (1973) - The Roman Thin Walled Pottery from Cosa (1948-1954), *Memoirs of the American Academy in Rome*, 32.

MacKenzie W.S. and Zussman J. (1974). The Feldspars. Manchester University Press, U.K.

Mayet Fr. (1975) - Les céramiques à parois fines dans la péninsule ibérique. Publications du Centre Pierre Paris. 1. Université de Bordeaux III, Centre Pierre Paris; diffusion, E. de Boccard, Talence, Paris.

Melluso L., Morra V., Brotzu P., Tommasini S., Renna M.R., Duncan R.A., Franciosi L. and d'Amelio. F. (2005) - Geochronology and petrogenesis of the cretaceous Antampombato-Ambatovy complex and associated dyke swarm, Madagascar. *Journal of Petrology*, 46, 1963-1996.

Melluso L., Srivastava R.K., Guarino V., Zanetti A. and Sinha A.K. (2010) - Mineral compositions and petrogenetic evolution of the ultramafic-alkaline - carbonatitic complex of Sung Valley, northeastern India. *The Canadian Mineralogist*, 48, pp. 205-229

Millet M. (1993) - Samian from the sea: Cala Culip shipwreck IV. *Journal of Roman Archaeology*, 6, 415-19.

Morra V., De Bonis A., Grifa C., Langella A., Cavassa L. and Piovesan R. (2013) - Minero-petrographic study of cooking ware and Pompeian Red Ware (Rosso Pompeiano) from Cuma (Southern Italy). *Archaeometry*, 55(5), 852-879.

Morimoto N. (1988). Nomenclature of pyroxenes. *Mineralogical Magazine*, 52, 535-550

Nodari L., Marcuz E., Maritan L., Mazzoli C. and Russo U. (2007) - Hematite nucleation and growth in the firing of carbonate-rich clay for pottery production. *Journal of the European Ceramic Society*, 27, 4665-73.

Renda G. (2004) - Il territorio di Caiatia. In: Carta archeologica e ricerche in Campania. *Atlante Tematico di Topografia Antica*, XV suppl., fasc. 1, Roma, pp. 237-423.

Ricci A. (1985) - Ceramica a pareti sottili. In: Atlante delle forme ceramiche II. Ceramica fine romana nel bacino mediterraneo (tardo ellenismo e primo impero), Roma, 231-357.

Scarsella F., Bergomi C. and Manganelli V. (1971) - Note illustrative della Carta Geologica d'Italia alla scala 1:100.000, Foglio 172 (Caserta), Servizio Geologico d'Italia.

Whitney D.I. and Evans B.W. (2010) - Abbreviations for names of rock-forming minerals. American Mineralogist, 95, 185-187